



Shearing Behavior at the Interface of Sand-Structured Surfaces Subjected to Monotonic Axial Loading

Mu'ath I. Abu Qamar ^{1*}, Mohammad F. Tamimi ¹, Ammar A. Alshannaq ¹,
Rama O. Al-Masri ¹

¹ Department of Civil Engineering, Yarmouk University, Irbid 21163, Jordan.

Received 24 June 2024; Revised 10 September 2024; Accepted 16 September 2024; Published 01 October 2024

Abstract

Enhancing the interface shear strength is crucial in the capacity and design of several geotechnical structures when subjected to static loading. The efficiency of these structures can be enhanced by utilizing innovative designs that allow the mobilization of higher interface shear resistance with bio-inspired-engineered or structured (rough) surfaces when compared to conventional smooth or random rough surfaces of the same geometry (i.e., soil-foundation contact area). Bio-inspired-engineered surfaces used in this study are developed after surfaces with snakeskin-inspired and engineered rough designs that maximize the interface shear resistance in cohesionless and cohesive soils. The frictional behavior and resistance of the bio-inspired-engineered surfaces were experimentally evaluated utilizing a modified interface direct shear apparatus on three locally available sand specimens. Results from tests on smooth surfaces against three different sands mobilized almost the same resistance and soil contraction. The results indicate a behavior significantly influenced by the shape and arrangement of the surface features, accompanied by larger resistance and volume dilation. A parametric study on the characteristics of the structured elements on three sands revealed the isolated impact of elements arrangement, shape, and roughness on the maximum attainable interface strength. The surface element characteristic ratio is found to control the load-transfer mechanism between sand and bio-inspired-engineered structured surfaces.

Keywords: Interface Shear Testing; Modified Direct Shear Device; Roughness; Sand-Structure Interface; Bio-Inspired Surfaces.

1. Introduction

Structural elements and geotechnical structures with load-carrying capacity that rely on interface friction can benefit from adopting innovative surface designs rather than conventional ones. These designs allow for the mobilization of higher interface shear resistance. The load-transfer mechanism across a soil-structure interface mainly occurs through friction between soil grains and a smooth or slightly randomly rough surface, or through passive resistance resulting from structured surface elements or a high level of roughness. These forces cause soil grains to displace under normal (confining) stress, with relative movement at the interface. The difference in design results in bearing stress applied to transverse surface elements that are normal to the direction of shearing [1, 2].

It is widely accepted that increasing the roughness of a surface leads to larger interface shear resistances. This confirms the significant role of surface roughness in the design and load-carrying capacity of geotechnical structures such as piles, reinforcing elements in mechanically stabilized earth walls, and soil nails and anchors [3–6]. However, previous studies have shown contradictory data, particularly regarding the maximum attainable interface shear strength [1, 7–10] and the

* Corresponding author: abuqamar.muath@yu.edu.jo

 <http://dx.doi.org/10.28991/CEJ-2024-010-10-06>



© 2024 by the authors. Licensee C.E.J, Tehran, Iran. This article is an open access article distributed under the terms and conditions of the Creative Commons Attribution (CC-BY) license (<http://creativecommons.org/licenses/by/4.0/>).

controlling parameters for different surface conditions, including maximum roughness, normalized roughness, and surface element characteristics [9, 11–14]. The role of the normalized roughness parameter (R_n), which is the ratio of maximum roughness to the mean particle size, on the shear behavior of a soil-random rough surface interface has been widely accepted by many researchers [6, 15–20]. On the other hand, other researchers suggest that the interface shear resistance of surfaces with bioinspired or periodic asperities is significantly influenced by the form, height, base length, and spacing between asperities [1, 7, 11, 21, 22]. However, its applicability requires further testing with different soil types.

Recently, several studies have focused on the interface shear behavior of rough surfaces in cohesionless and cohesive soils under cyclic axial loading [7, 23–26]. To enhance the interface shear resistance of geotechnical structures, various design proposals have been made, including ribbed, machined, bio-inspired, or idealized surfaces [9, 27–31]. However, compared to the numerous experimental studies that have investigated the interface shear behavior, the number of numerical simulations available in the literature is limited. For example, Wang et al. [32] compared interface shear test results to simulations using the Mohr-Coulomb and hypoplasticity models in cohesive soils. Stutz and Martinez [33] used a hypoplasticity interface and soil model to simulate the interface between sand and surfaces of varying roughness, and compared the simulation results to experimental data from several axisymmetric interface shear tests. Zhou et al. [34] simulated the pull-out behavior of soil nails in a pull-out box under different overburden pressures using a three-dimensional (3D) finite element (FE) model in ABAQUS software.

In the field of bioinspired geotechnics, recent research studies [21, 30, 35, 36] have suggested that the load-carrying capacity of piles under axial loading could benefit from adopting designs inspired by the ventral scales of snakeskin. O'Hara and Martinez [26], who performed interface shear tests on surfaces with idealized snakeskin profiles obtained from 3D scans of preserved snake scales, observed that surfaces inspired by snakeskin had higher interface strength than conventional surfaces. They also concluded that snakeskin-inspired profiles mobilized significant frictional anisotropy, where shearing in the cranial direction generated larger shear stresses than shearing in the caudal direction. Martinez et al. [35] and Martinez [37] conducted monotonic and cyclic pull-out tests on piles with snakeskin-inspired surfaces, suggesting that these surfaces create direction-dependent interface strength and soil volume changes. Martinez and O'Hara [38] developed direction-dependent failure envelopes for sand-structure interfaces with snakeskin-inspired surfaces by performing monotonic interface shear tests. A recent study by Martinez et al. [39] presented the results of field load tests on anchorage elements with snakeskin-inspired surfaces. It was found that the tested elements did not require grout and reduced the force needed for installation.

This paper presents a study on the interface behavior of bio-inspired engineered or structured (rough) surfaces with trapezoidal-like elements sheared against sandy soils of different particle sizes under monotonic axial loading. The study evaluates the concept of using bio-inspired engineered surfaces to enhance interface shear resistance. The experimental program involved modifying the conventional direct shear test apparatus to perform a series of interface shear tests. This paper summarizes the results of interface direct shear tests on sandy soil, both smooth and structured (rough), with variable clear distances between elements of constant roughness (i.e., different element characteristic ratios). The particle sizes of the soil were varied to examine whether the interface shear resistance of bio-inspired engineered or structured (rough) surfaces is solely controlled by the geometry and form of surface elements or if it is also influenced by the normalized roughness parameter.

2. Experimental Setup

2.1. Modified Interface Direct Shear Apparatus

In this study, a conventional direct shear test device (MATEST, Italy) was modified to allow for conducting both conventional direct shear tests and interface direct shear tests. Figure 1 presents a schematic diagram of the direct shear apparatus, showing all of its components. The UTM II software, developed by MATEST, is used to define the shear test parameters, including shearing rate, horizontal stroke, and test type. The UTM II software also enables simultaneous logging of sensor readings, which include horizontal shear force, horizontal (shearing) displacement, and vertical (volume change) displacement. As shown in Figure 1, the direct shear test apparatus is equipped with an S-shaped load cell and two linear (spring-based) potentiometers to measure interface shear resistance at both the soil-soil and soil-surface interfaces, as well as horizontal and vertical displacements during testing. The load cell has a capacity of 3,000 N, while the measuring range of the horizontal and vertical potentiometers is 25.4 mm and 15.7 mm, respectively. Normal stress is applied to the sample by placing dead weights on a lever arm with a 1:10 ratio. The configuration of the device only allows for performing conventional and interface direct shear tests under constant normal load (CNL) boundary conditions. A reaction arm (frame) ensures the full transfer of the frictional resistance mobilized at the soil-soil and soil-surface interfaces to the S-shaped load cell. The mobilized shear stress at the interface is determined by dividing the directly measured shear force by the sample's cross-sectional area. The stress ratio is calculated by dividing

the mobilized shear stress by the normal (confining) stress applied to the sample or surface during the test. The cross-sectional area of both the soil-soil samples and the soil-surface contact area is 60 mm × 60 mm. The apparatus allows for conventional and interface shear tests at displacement shearing rates ranging from 0.00001 mm/min to 10 mm/min.

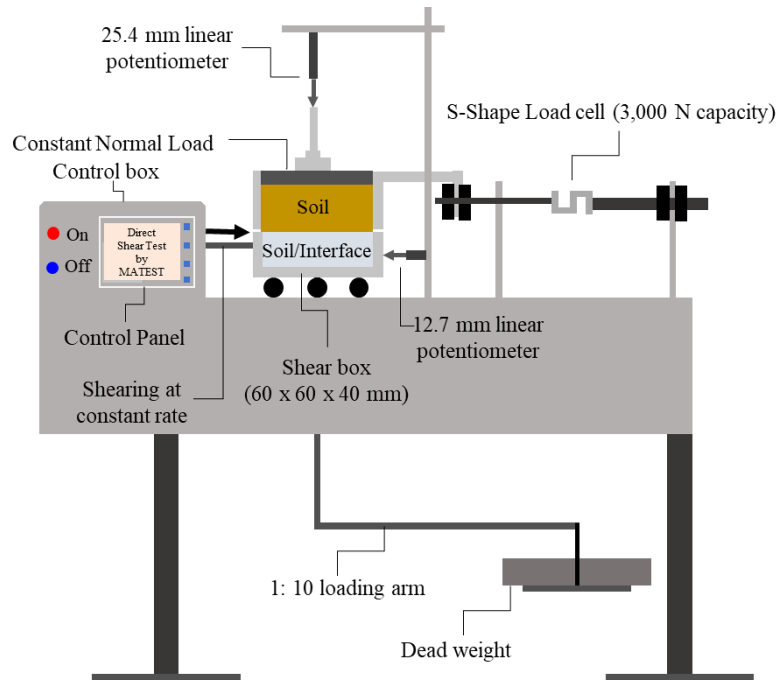


Figure 1. A Schematic of the direct shear tests (DST) apparatus used in the present study

Research studies conducted by DeJong & Westgate [40], Martinez & Palumbo [36], and Han et al. [16] involved the modification of conventional direct shear tests to perform interface shear testing. The modified apparatus was adjusted to test smooth, randomly rough, and bio-inspired surfaces against sandy soils under static and cyclic axial loading [12, 30, 40, 41]. The thickness of the top and bottom halves of the shear box is 40 mm, as illustrated in Figure 1. To investigate the influence of structured (rough) or bio-inspired-engineered surfaces on interface strength, the shear box of the conventional shear device (see Figure 2) was modified to allow for interface shear tests. The bottom half of the box, which contains the soil specimen in conventional direct shear tests, was adapted to accommodate surface blocks (cuboids) with different designs, in addition to the smooth surface condition. The dimensions of the interface material block are 60 mm × 60 mm × 20 mm. Figure 2 shows the modified shear box with smooth and structured (rough) surfaces.

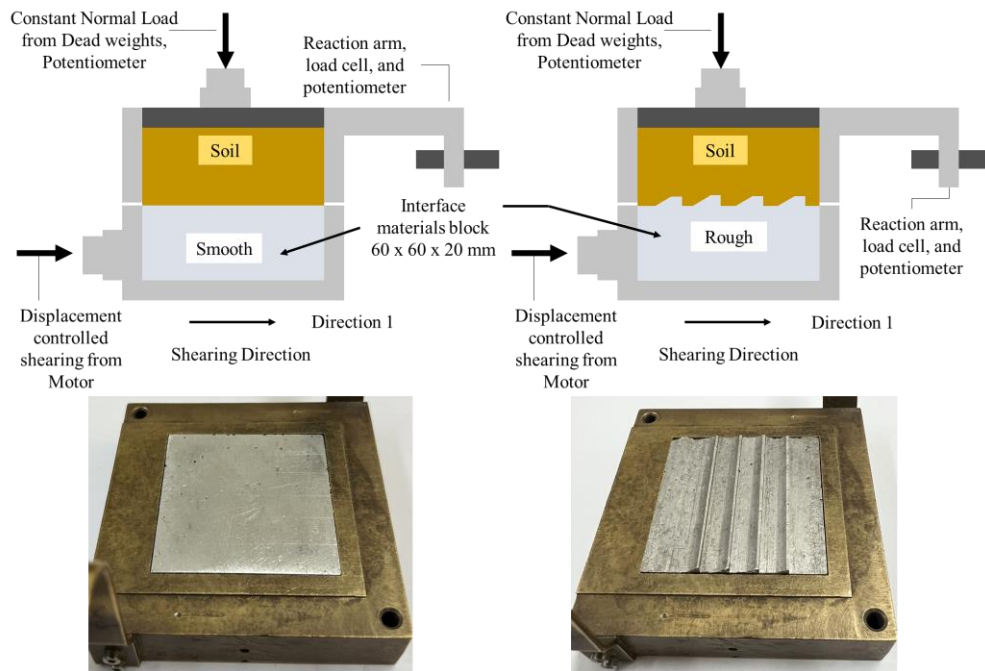


Figure 2. Schematic and actual photographs of modified interface shear box for soil-smooth and soil-structured (rough) interface conditions showing direction of shearing

Research studies available in the literature have adopted either a soil-over-solid surface or solid surface-over-soil setup (or shear mode) to perform interface shear tests [12, 14, 30, 42, 43]. The majority of the studies used the soil-over-solid surface or lower-shear plate shear mode to modify conventional direct shear test apparatus. As in conventional direct shear tests, the top shear box containing the soil remained stationary, while the bottom half of the shear box moved horizontally at a constant shearing rate of 0.5 mm/min, with a total displacement of 4 mm in both conventional and interface direct shear tests.

2.2. Test Surface Characteristics and Design

A total of five surfaces, a smooth and four bio-inspired-engineered structured (rough) surfaces, were tested against three locally available sandy soils as part of this research study. All surfaces were manufactured from aluminum in the engineering workshops at Yarmouk University. The smooth surface was treated and polished to achieve the required level of roughness, ensuring that the load-transfer mechanism was governed by particle sliding under the relative movement between soil and surface. Several research studies have focused on the influence of surface roughness (expressed in terms of normalized roughness parameters) on interface shear behavior and response in both cohesionless [9] and cohesive soils [11, 27].

Martinez & Frost [9] conducted laboratory experiments on friction sleeves using both smooth and rough sleeves, with surface roughness up to 2.0 mm, and confirmed the significant role of surface roughness in the strength of sand-material interfaces. Abu Qamar and Suleiman [7] investigated the influence of surface element height (up to 1.75 mm) using 3D-printed surfaces on the strength of cohesive soil-material interfaces, utilizing a recently modified cyclic interface shear test system [23]. Both studies showed agreement with existing literature and concluded that the strength of both cohesionless and cohesive soil-structure interfaces increases with surface roughness, potentially matching the internal strength of the interface soils. The bio-inspired-engineered surfaces (also referred to as structured or rough surfaces) were manufactured with trapezoidal-like elements placed at variable clear distances (D) up to 55 mm and a maximum roughness (R_{max}) of 2.0 to maximize interface strength.

As illustrated in Figure 3, each trapezoidal-like element has a base length of 5 mm, with a 1 mm smooth (untextured) crest (top) segment, resulting in an element angle of 26.56° . During axial loading, the shape of the element allows for mobilizing interface shear resistance (friction) at the crest (top) and untextured length between elements. Additional shear resistance could be mobilized due to the development of passive soil wedges at the right-angle side of the element. The structured surface elements are spaced at clear distances (D) of 55 mm (Rough I), 25 mm (Rough II), 15 mm (Rough III), and 10 mm (Rough IV), respectively. The clear distance between elements was varied to examine its influence on mobilized shear resistance, with the maximum distance limited to 55 mm due to the shear box size. According to ASTM D5321-21, the standard recommends using a shear box with dimensions of 305 mm by 305 mm to minimize the effects on measured response [44]. To minimize boundary effects on the measured responses, smooth (untextured) zones, approximately 10 mm in length, were created on both ends of the structured (rough) surfaces (see Figure 3). Previous researchers investigating the behavior of soil-structured interfaces using modified direct shear test devices have used 11 mm length untextured ends to minimize boundary effects [45, 46]. Monotonic interface shear tests were performed against surfaces with the same roughness but varying clear distances to investigate the effects of bio-inspired-engineered surface element geometry on strength and behavior in sandy soils.

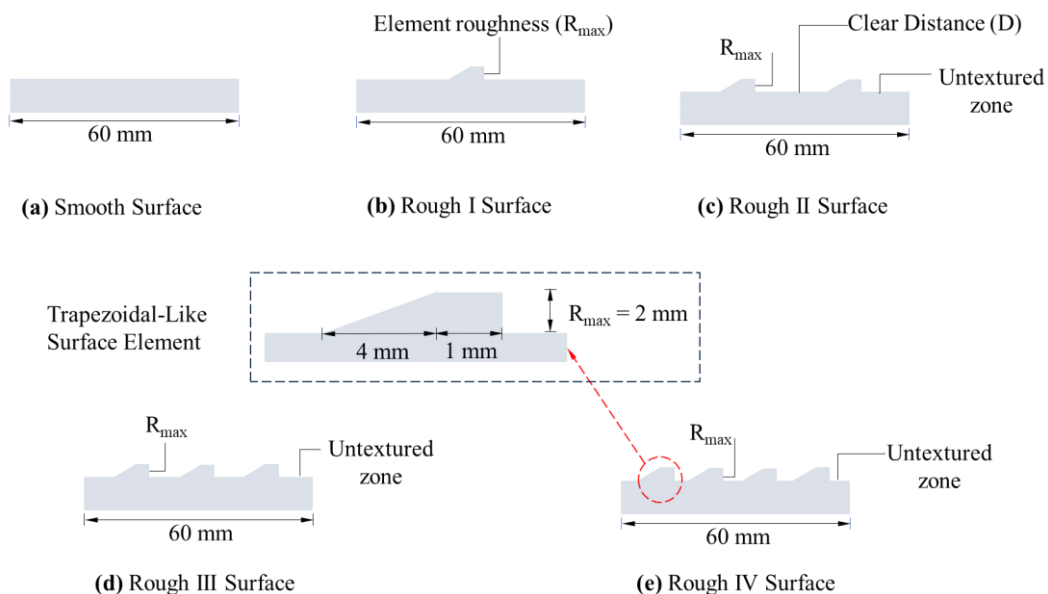


Figure 3. Details of smooth and structured (rough) surfaces design

3. Test Soil Properties and Preparation

3.1. Soil Properties

Three locally available sandy soils were used in this study to examine the influence of particle size on the interface shear resistance of structured (rough) surfaces. To facilitate the interpretation of the results for each soil, the three quartz-based soils are labeled as Soil 1, Soil 2, and Soil 3. The particle size distribution (PSD) curves for the soils were developed according to ASTM D6913/D6913M-17 [47]. The PSD curves for Soil 1, Soil 2, and Soil 3, along with their actual photographs, are shown in Figure 4. The mean particle diameters (D_{50}) of Soils 1, 2, and 3 are 0.32 mm, 0.58 mm, and 0.70 mm, respectively. Table 1 provides a summary of key properties, including the mean particle size (D_{50}), maximum and minimum void ratios (e_{max} , e_{min}), coefficient of uniformity (C_u), and coefficient of curvature (C_c). According to the Unified Soil Classification System (USCS), all three sands are classified as poorly-graded (SP) sands (see Table 1) [48].

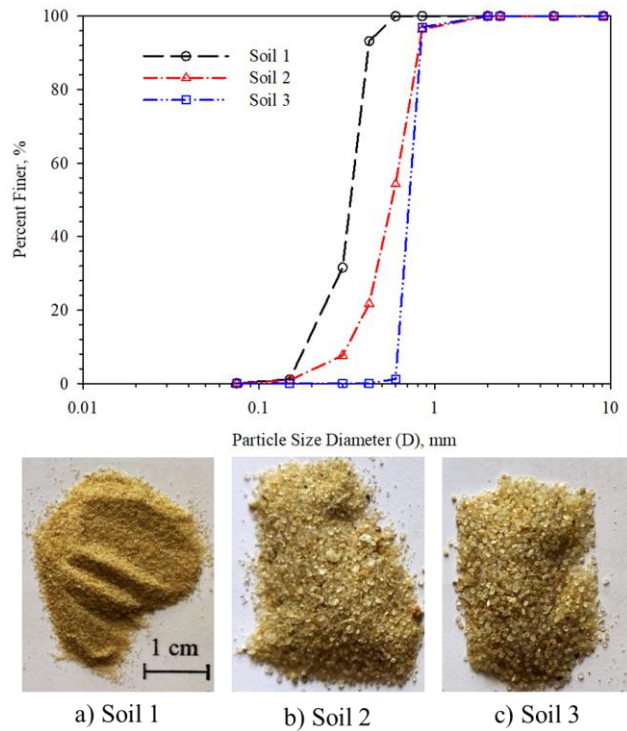


Figure 4. Particle size distribution (PSD) curves and photos for the soils used in this study

Table 1. Summary of properties of the soils used in this study

Property	Soil 1	Soil 2	Soil 3
Coefficient of uniformity (C_u)	1.89	1.94	1.16
Coefficient of curvature (C_c)	1.28	1.07	0.95
Median particle size (D_{50})	0.32	0.58	0.70
Specific gravity (G_s)	2.58	2.64	2.61
Maximum void ratio (e_{max})	0.869	0.811	0.881
Minimum void ratio (e_{min})	0.558	0.541	0.567
Unified Soil Classification System (USCS)	SP*	SP*	SP*

* SP: Poorly graded sand with little or no fines.

3.2. Soil Specimen Preparation

Representative soil specimens used for all conventional direct shear and interface shear tests were prepared with the same target relative density (D_r). The specimens measured 60 mm in length and 60 mm in width, which is approximately 86 times the maximum particle diameter (0.7 mm) of the coarse sand used in the tests (see Table 1). This size exceeds the minimum sample size of $10D_{max}$ as prescribed by ASTM D3080/D3080M-11 [49]. The specimen height ranged from 36 to 38 mm for conventional direct shear tests and from 18 to 20 mm for interface direct shear tests. For interface shear tests, all sand specimens were air-pluviated into the top half of the shear box, placed over smooth and bio-inspired-engineered (or structured) surfaces, to achieve a target relative density (D_r) of $70 \pm 1\%$. Before applying normal stress,

the gap between the top and bottom halves of the shear box was adjusted to be approximately equal to the largest sand particle in the specimen [49].

The internal friction angles of test soils 1, 2, and 3 were determined by conducting a series of conventional direct shear tests on representative soil samples. The configuration of the conventional direct shear tests for performing soil-soil strength tests is shown in Figure 1. These tests were conducted under a range of normal (confining) pressures to develop the Mohr-Coulomb failure envelope. The peak internal shear strength of each soil was determined at the corresponding normal (confining) stress. Figure 5 displays the peak failure envelopes for soils 1, 2, and 3. As shown in Figure 5, the internal friction angles for soils 1, 2, and 3 are 34.9° , 33.2° , and 37.9° , respectively. The tests were performed on representative samples prepared with a target relative density of 70%.

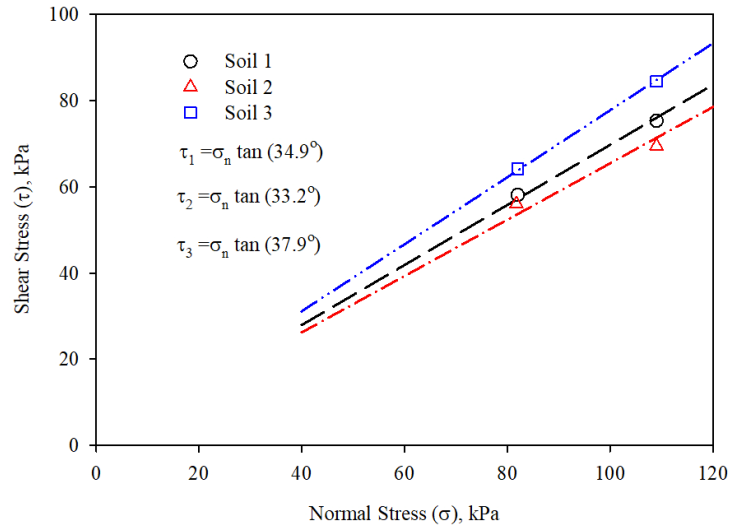


Figure 5. Mohr-Coulomb failure envelop for soils 1, 2, and 3 from conventional direct shear tests on representative specimens

4. Results and Discussion

The interface shearing behavior and resistance of all three soils (1, 2, and 3) tested against smooth and structured (rough) surfaces under axial monotonic loading were experimentally evaluated. This includes the interface shear resistance against smooth surfaces, the interface resistance of structured (rough) surfaces with different characteristics sheared against the soil, and the load transfer mechanism at sand-smooth and sand-structured (rough) interfaces. The impact of surface element characteristics on interface resistance is then discussed.

4.1. Shear Response at Soil-Smooth Interface Condition

The modified interface direct shear test device was used to conduct three interface shear tests on smooth surfaces with soils 1, 2, and 3. The results from these tests, conducted at a normal (confining) stress of 50 kPa and a target relative density of 70%, are shown in Figure 6. Figure 6 compares the shear stress and the shear stress to normal stress (τ/σ) ratio with horizontal displacement (Δ) for the three different soil samples tested against the smooth interface condition at a shearing rate of 0.5 mm/min. Figure 6-a demonstrates that all soil samples show an increase in shear stress with horizontal displacement up to approximately 0.5 mm, followed by a decrease in shear stress with further displacement. The post-peak shear stress versus horizontal displacement curves for soils 1 and 2 exhibit a slight reduction before stabilizing with displacement. However, the interface shear stress versus horizontal displacement curve for Soil 2 shows a more pronounced reduction from peak to post-peak stress. The difference in the observed resistance can likely be attributed to variations in soil composition, density, internal angle of friction, and particle size distribution. The peak interface shear resistance mobilized at the smooth surface against soils 1, 2, and 3 were 19.2 kPa, 19.0 kPa, and 19.3 kPa, respectively. The post-peak interface shear resistance for soils 1, 2, and 3 were 15.0 kPa, 16.0 kPa, and 13.3 kPa, respectively. In Figure 6-b, the peak stress ratio (τ/σ) for all soils ranges from 0.37 to 0.38, while the post-peak stress ratio ranges from 0.26 to 0.32. The peak interface friction angles (δ_p) for soils 1, 2, and 3 at the smooth interface are 20.33° , 20.73° , and 20.63° , respectively, which correspond to interface to internal angle of friction ratios $(\delta/\phi)_p$ of 0.58, 0.54, and 0.62 for the three soils. The post-peak interface to internal angle of friction ratios $(\delta/\phi)_{pp}$ were 0.42, 0.40, and 0.55 for the three soils, respectively. Contractive behavior was observed in tests on the smooth surface sheared against all soils, caused by particle sliding and the load transfer mechanism occurring at the soil-smooth interface under monotonic axial loading. The findings of the current study are consistent with measurements made by other researchers on the development of negligible shear zone deformation at soil-smooth surface interfaces [22, 50, 51].

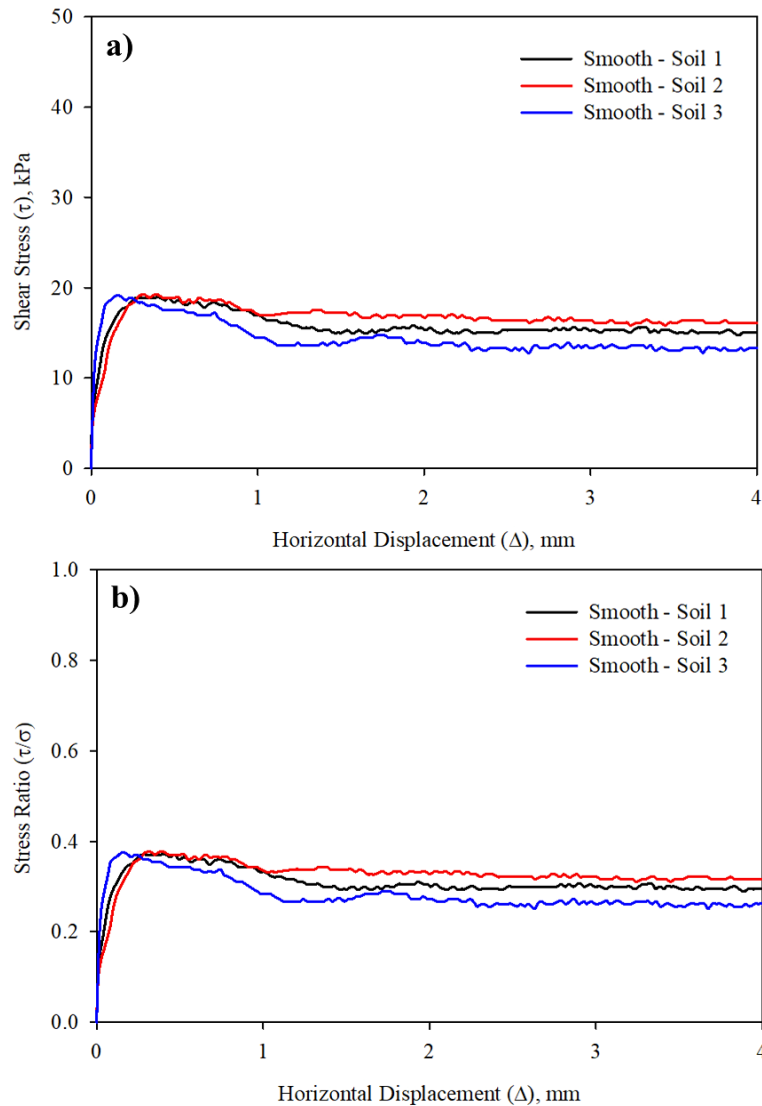


Figure 6. Results of interface shear tests on soils 1-, soil 2-, soil 3-smooth surface interface condition: (a) measured interface shear stress vs. horizontal displacement (Δ), and (b) corresponding shear stress to normal stress ratio (τ/σ) as function of horizontal displacement (Δ), interface tests conducted at 50 kPa normal (confining) stress.

4.2. Shear Resistance of Soil-Structured (Rough) Surface Interface

The mobilized interface shear resistance, reported in terms of shear stress (τ) with horizontal displacement, during interface direct shear tests performed against smooth (no surface elements) and structured (rough) surfaces with trapezoidal-like elements placed at different spacings, is presented in Figure 7. Figure 7 shows the response curves for smooth (no elements), Rough I (one element), Rough II (two elements), Rough III (three elements), and Rough IV (four elements) surfaces sheared against Soil 1 prepared at 50 kPa. As previously discussed, the smooth surface curve shows peak resistance at a displacement of less than 0.5 mm, followed by a strain-softening response. The response curves for structured (rough) surfaces show that the mobilized resistance increases as the level of roughness, in terms of the number of elements, increases. As previous research has shown, the mobilized shear strength and behavior of soil-structure interfaces are significantly impacted by surface roughness and the internal friction of the sand. The findings of the present study are consistent with measurements made in earlier studies [13, 52–57]. Unlike the soil 1-smooth interface shear response, the peak interface shear stress of structured (rough) surfaces increases up to approximately 1.0 mm of horizontal displacement, then stabilizes with a minimal decrease in resistance. The results (see Figure 7) show that the measured interface shear resistance increases with the number of surface elements (or the level of roughness) for Rough I, II, and III, while lower interface strength is mobilized for Rough IV.

The influence of roughness on interface resistance is evident, as the strength of the soil-structured (rough) surfaces increases by 96%, 134%, 147%, and 111% of the sand-smooth strength, corresponding to peak shear stress to normal stress (τ/σ) ratios of 0.73, 0.87, 0.91, and 0.78, respectively. These results are consistent with the limited understanding

of the behavior of structured (rough) surfaces, where the characteristics of surface elements (roughness, form, distance) play a critical role in the response and behavior of soil-structure interfaces. Unlike structured or ribbed surfaces, the interface shear resistance of sand-random rough surfaces is mainly affected by roughness parameters (e.g., the average roughness (R_a), maximum roughness (R_{max}), normalized roughness ($R_n = R_{max}/D_{50}$), and relative roughness ($R = R_a/D_{avg}$) first proposed by Uesugi & Kishida (1996) to describe surface roughness. The normalized roughness parameter (especially R_n), a measure of relative roughness to mean particle size, has been widely used in studies focused on the response and behavior of sand-structured interfaces [9, 15, 19, 24, 58].

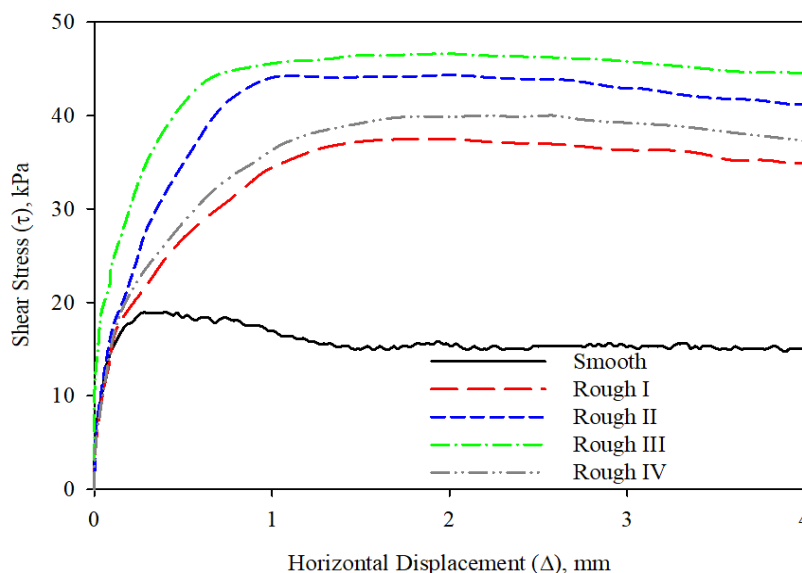


Figure 7. Results of interface shear tests of smooth and structured (rough) surfaces sheared against soil 1 in direction 1: measured interface shear stress vs. horizontal displacement (Δ), interface tests conducted at 50 kPa normal (confining) stress

Figure 8 shows the peak interface shear stress for smooth and structured (rough) surfaces, with the clear distance between trapezoidal elements and the clear distance normalized to the maximum roughness of the elements (i.e., 2 mm). As observed in Figure 8-a, the interface shear resistance correlates with the clear distance between elements (D). As the distance between the elements increases (i.e., fewer elements within the gauge length), the interface shear resistance initially increases until it reaches a maximum value and then decreases. It is expected that the interface shear resistance will eventually decrease until it matches the resistance of the smooth surface condition (see Figure 8-a). The smooth surface interface strength is mainly due to frictional resistance from the sliding of soil particles during the relative movement between the soil and surface. Due to the design of the surface elements used in this study (i.e., trapezoidal-like elements), frictional resistance develops at the zone in front of and at the crest (top) of the elements, in addition to the formation of soil wedges at the faces of the elements through bearing stress applied to the transverse surfaces, normal to the direction of movement. It is important to note that the size of the elements affects the size of the soil passive wedge, with higher resistance achieved when surfaces allow the development of the maximum number of wedges, along with frictional resistance along the smooth (or untextured) zones.

The load transfer mechanisms between soils and various soil reinforcement systems, involving friction and/or passive resistance, have been described and further elaborated in several studies [1, 2, 7, 17, 22]. The observed results regarding the contribution of passive resistance to the total interface shear resistance are consistent with the test results reported in previous studies on interface shear behavior with periodic surfaces [1, 17, 22, 54]. Shearing against Soil 1 in direction 1 (see Figure 8-a) on structured (rough) surfaces developed confined soil wedges at the leading front of the right-angle side of the elements, combined with soil dilation, resulting in a local increase in normal (confining) effective stress with horizontal displacement. Figure 8-a suggests that a surface with 2 mm maximum roughness and a clear distance (D) of 15 mm achieves higher interface shear stress due to the development of more passive wedges, in addition to frictional resistance along the smooth (untextured) zones. As concluded by previous studies, the mobilized interface shear resistance is significantly influenced by surface roughness [5, 9, 13, 17, 27, 30]; therefore, the influence of the maximum roughness of structured (rough) surfaces on the mobilized interface shear resistance is not considered here.

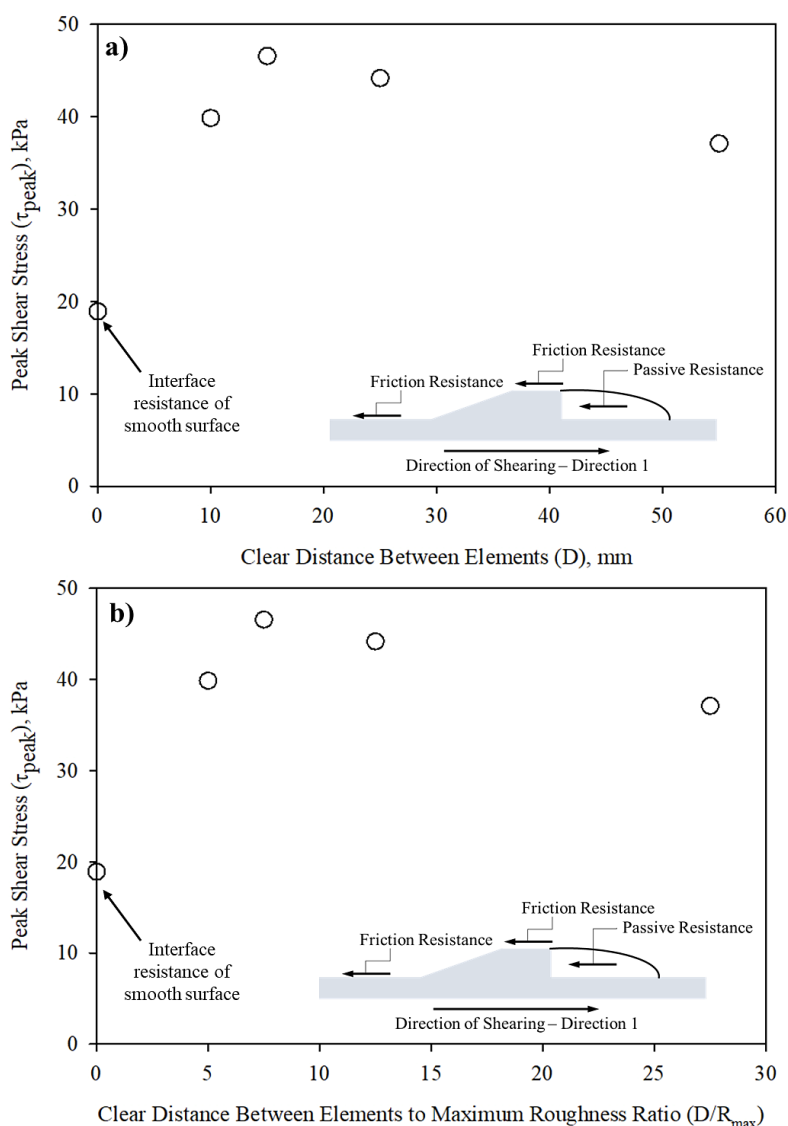


Figure 8. Results of interface shear tests of smooth and structured (rough) surfaces sheared against soil 1 in direction 1: a) relationship between peak interface shear stress and clear distance between surface elements, and b) relationship between peak interface shear stress and clear distance between surface elements to maximum roughness ratio, interface tests conducted at 50 kPa normal stress.

he maximum roughness (R_{max}) and the clear distance (D) between surface elements of bio-inspired engineered surfaces also influence the mobilized interface shear stress and soil volume change. The ratio of clear distance to maximum roughness (D/R_{max}) was introduced to study the relationship between this ratio (or element characteristics) and the load transfer mechanism of structured (rough) surfaces. Surfaces with a small D/R_{max} ratio are more likely to mobilize small soil wedges with minimal friction, whereas surfaces with a large D/R_{max} ratio tend to mobilize fewer soil wedges and exhibit a friction-dominated resistance. Therefore, a surface design with an optimal D/R_{max} ratio could allow the development of the maximum number of soil wedges, in addition to frictional resistance on the smooth (untextured) zone between the elements and the element crest (top). The results of all interface shear tests on soil 1 are plotted as a function of the D/R_{max} ratio in Figure 8. As shown in Figure 8-b, the D/R_{max} ratio seems to influence the maximum attainable interface shear resistance and soil dilation of structured (rough) surfaces. The Rough III surface, with a D/R_{max} ratio of 7.5, resulted from a clear distance of 15 mm and a maximum roughness of 2 mm, while other structured (rough) surfaces mobilized lower resistance. These results are consistent with the findings reported by Martinez et al. [21] from interface shear tests on snakeskin-inspired surfaces in sandy soils.

To confirm the relationship between the characteristics of bio-inspired engineered surfaces and the observed load-transfer mechanism, a series of interface direct shear tests were performed on two soils, labeled Soil 2 and Soil 3. Figure 9 presents the response curves for smooth (no elements), Rough I (one element), Rough II (two elements), Rough III (three elements), and Rough IV (four elements) surfaces sheared against Soil 2, prepared at 50 kPa. The figure shows that the soil 2-smooth interface shear response peaks at approximately 0.5 mm, followed by slight strain softening with horizontal displacement. In contrast, the peak interface shear stress for structured (rough) surfaces increases up to

approximately 1.0 mm, then stabilizes with minimal decrease in resistance. The results in Figure 9 demonstrate that the measured interface shear resistance increases with the number of surface elements (or level of roughness) for Rough I, II, and III, while Rough IV mobilizes lower interface strength, consistent with the responses observed during tests on Soil 1. The Rough III interface sheared against Soil 2 yielded the highest interface shear resistance among the rough surfaces, although the mobilized peak interface shear stress for Soil 2 was slightly lower than that for Soil 1. This difference in mobilized peak interface shear resistance is attributed to the difference in the internal angle of friction between Soils 1 and 2. The influence of roughness on the interface resistance is evident, as the soil-structured (rough) surfaces exhibit an interface strength of 77%, 95%, 103%, and 89% of the smooth sand strength, corresponding to peak shear stress to normal stress (τ/σ) ratios of 0.66, 0.73, 0.77, and 0.71, respectively.

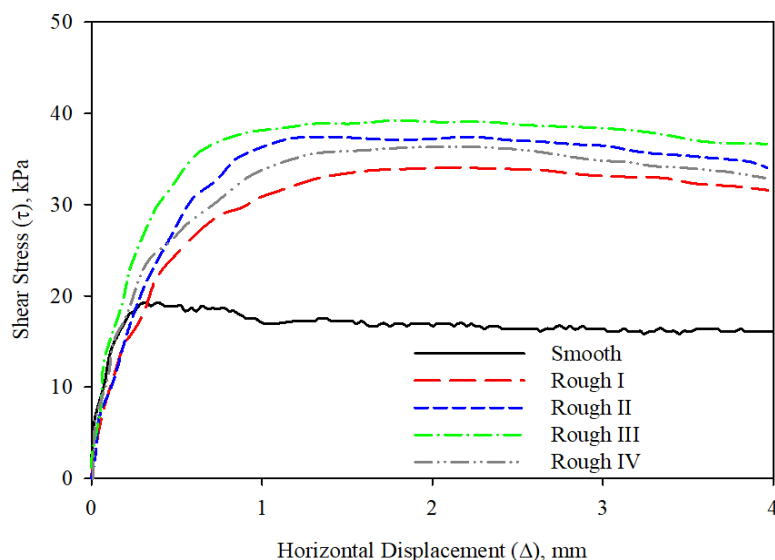


Figure 9. Results of interface shear tests of smooth and structured (rough) surfaces sheared against soil 2 in direction 1: measured interface shear stress vs. horizontal displacement (Δ), interface tests conducted at 50 kPa normal (confining) stress

A comparison of the trends obtained in this study suggests that the D/R_{\max} ratio impacts the load-transfer mechanisms of sand-structured (rough) surfaces, including the development of passive wedges due to surface element roughness, the clear distance between elements, and soil dilation during soil-surface relative movement. As suggested by previous research, the load-transfer mechanism and interface shear resistance for surfaces with random roughness, resulting from abrasion or artificial roughening, are well described and controlled by the normalized roughness parameters (e.g., R , R_a , R_n) [9, 42, 52, 57].

Figure 10 shows the mobilized peak interface shear stress for smooth and structured (rough) surfaces, with both the clear distance and the clear distance normalized to the maximum roughness of the elements. As seen in Figure 10-a, the interface shear resistance correlates with the distance (D). As the clear distance increases, the interface shear resistance rises until it reaches a maximum value and then decreases. A smaller distance implies a larger number of elements per unit of contact length, whereas the interface shear resistance of surfaces with larger clear distances decreases until it matches the smooth surface resistance (see Figure 10-a). Shearing against Soil 2 in direction 1 (see Figure 3) with structured (rough) surfaces led to the possible development of passive wedges (or passive resistance) in addition to friction resistance, combined with soil dilation. Figure 10-a suggests that the Rough III surface, with a clear distance of 15 mm and a constant maximum roughness of 2 mm, yielded higher resistance compared to smooth and other structured (rough) surfaces.

Results from interface direct shear tests conducted on Soil 2 against smooth and structured (rough) surfaces are depicted with the D/R_{\max} ratio in Figure 10-b. As shown in Figure 10-b, the D/R_{\max} ratio appears to control the maximum attainable resistance of structured (rough) surfaces. The Rough III surface has a D/R_{\max} ratio of 7.5, while Rough I, II, and IV structured (rough) surfaces, with D/R_{\max} ratios of 5, 12.5, and 27.5, mobilized lower resistance.

The results of the interface direct shear tests on Soil 3 are shown in Figure 11. Soil 3 is coarser compared to Soils 1 and 2, with a D_{50} of 0.70 and C_u and C_c values of 1.16 and 0.95, respectively. Based on the particle size distribution curves presented in Figure 4, Soil 3 is a poorly graded soil (composed of single-sized particles) and has a relatively high internal angle of friction. Figure 11 demonstrates that, compared to the Soil 3-smooth interface resistance, the structured (rough) surface exhibited higher resistance, with the resistance increasing with the level of roughness or the number of elements. The number of elements per unit length of contact is not the only factor influencing the mobilized resistance. For instance, Rough III, which has three elements, attains higher strength than Rough IV, which has four elements. The soil-structured (rough) surfaces achieved interface strengths of 89%, 119%, 131%, and 99% of the sand-smooth strength, corresponding to peak shear stress to normal stress (τ/σ) ratios of 0.71, 0.83, 0.87, and 0.75, respectively.

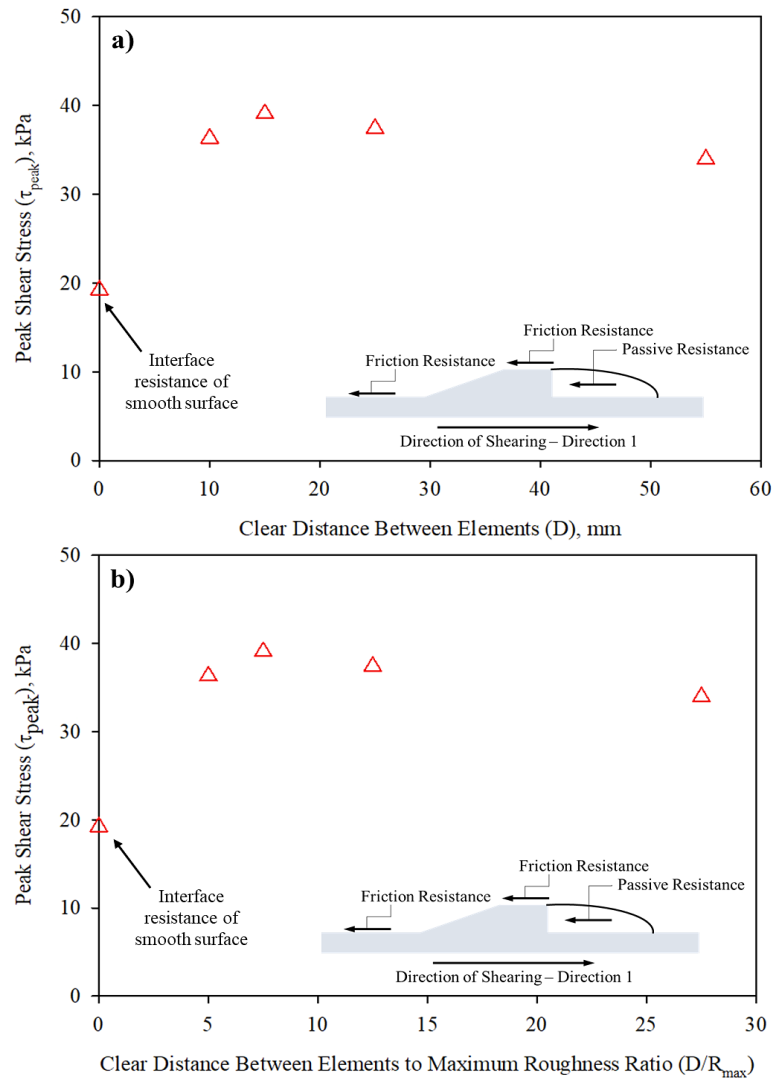


Figure 10. Results of interface shear tests of smooth and structured (rough) surfaces sheared against soil 2 in direction 1: a) relationship between peak interface shear stress and clear distance between surface elements, and b) relationship between peak interface shear stress and clear distance between surface elements to maximum roughness ratio), interface tests conducted at 50 kPa normal (confining) stress.

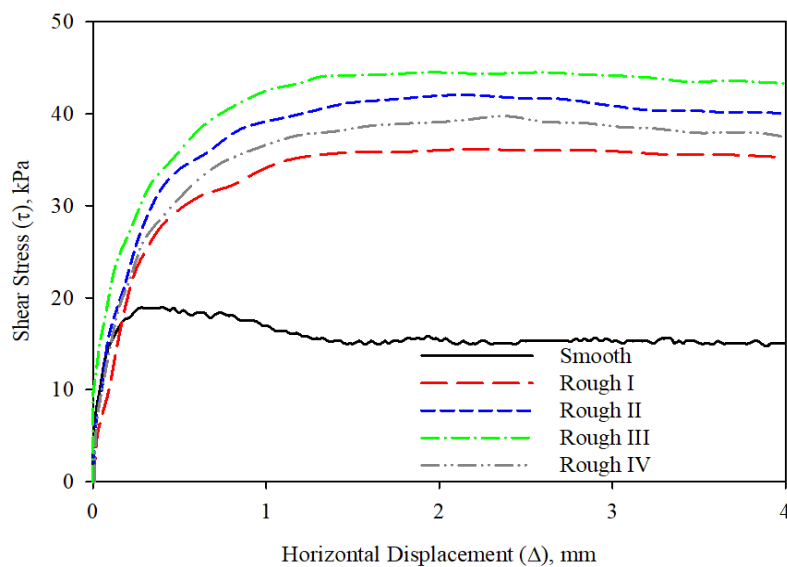


Figure 11. Results of interface shear tests of smooth and structured (rough) surfaces sheared against soil 3 in direction 1: measured interface shear stress vs. horizontal displacement (Δ), interface tests conducted at 50 kPa normal (confining) stress

Figure 12 shows the mobilized peak interface shear stress for both smooth and structured (rough) surfaces, with clear distance and clear distance normalized to the maximum roughness of the elements. As shown in Figure 12-a, the interface shear resistance is related to the distance (D). The maximum attainable shear resistance occurred when Rough III was tested against Soil 3, with a clear distance of 15 mm. This maximum shear resistance represents an increase of 131% compared to the Soil 3-smooth surface interface resistance, with a shear stress to normal stress ratio of 0.87.

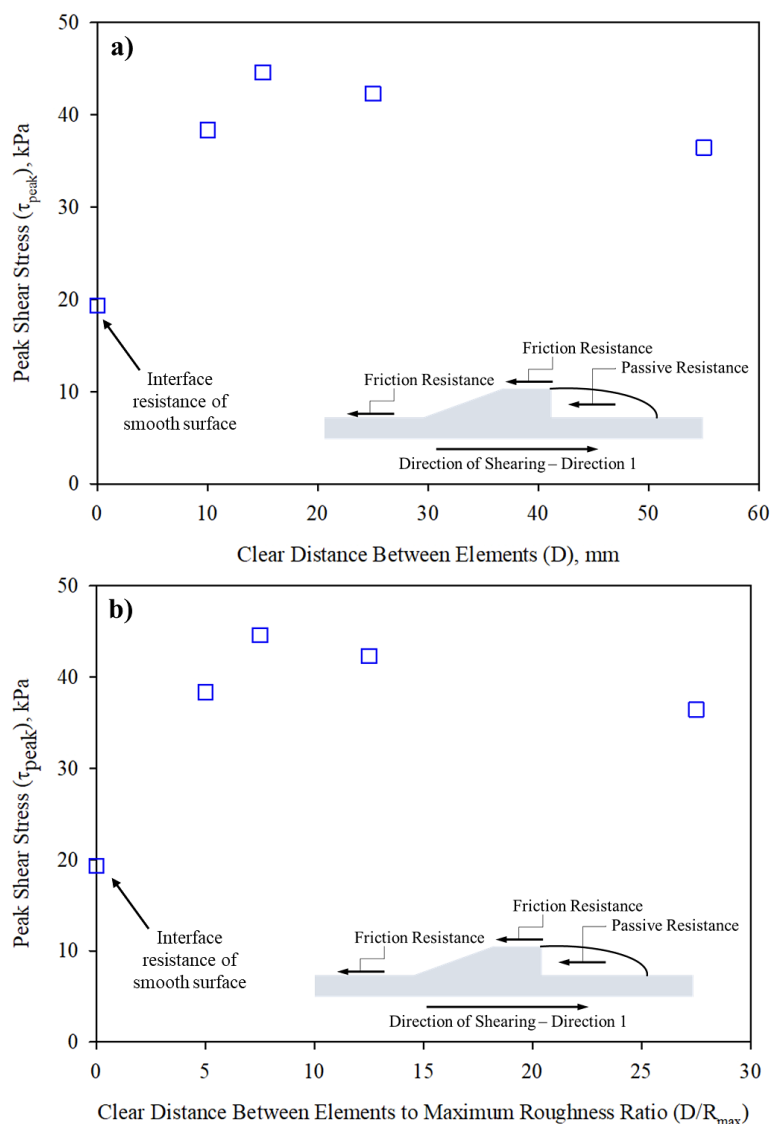


Figure 12. Results of interface shear tests of smooth and structured (rough) surfaces sheared against soil 3 in direction 1: a) relationship between peak interface shear stress and clear distance between surface elements, and b) relationship between peak interface shear stress and clear distance between surface elements to maximum roughness ratio), interface tests conducted at 50 kPa normal (confining) stress.

Figure 12-b confirms that the D/R_{max} ratio governs the load-transfer mechanism and the development of passive wedges. As mentioned earlier, Rough III (with a clear distance of 15 mm and a maximum roughness of 2 mm) achieved the maximum interface resistance, which supports the results in Figures 7-10. Unlike surfaces with random roughness, the interface behavior and resistance of structured (rough) surfaces are primarily controlled by the D/R_{max} ratio rather than the normalized roughness parameters. The trends observed here are consistent with the data reported by Martinez et al. [21].

4.3. Role of Structured Elements Characteristics on Interface Shear Resistance

A parametric study was conducted to investigate the effect of structured element characteristics, specifically maximum roughness (R_{max}) and the clear distance between elements (D), on the mobilized interface shear resistance of three different soil gradations (i.e., Soils 1, 2, and 3). Increasing the clear distance (D) while keeping the maximum roughness (R_{max}) constant at 2.0 mm led to higher mobilized shear resistances and greater interface soil dilation for all tested soils.

Figure 13 illustrates the relationship between the mobilized peak interface shear resistance of structured (rough) surfaces and the peak resistance of smooth surfaces, expressed as the peak shear stress ratio ($\tau_{peak}/\tau_{smooth}$). As shown in Figure 13, increases in the clear distance to maximum roughness (D/R_{max}) ratio led to higher peak shear stress ratios in tests on all three sandy soils. For Soil 1, which has a smaller D_{50} , an initial increase in D from 10 to 15 mm (corresponding to a D/R_{max} ratio of 5 to 7.5) resulted in a sharp increase in the mobilized shear stress ratio. Further increases in D from 15 to 25 mm (corresponding to a D/R_{max} ratio of 7.5 to 12.5) led to a moderate decrease in the shear stress ratio and increases from 25 to 55 mm (corresponding to a D/R_{max} ratio of 12.5 to 27.5) caused a more pronounced decrease in the stress ratio. The trends for tests with Soil 2 (medium) and Soil 3 (coarser) sands were somewhat similar to those observed for tests with Soil 1 (finer) sand. As seen in Figure 13, the interface shear resistance of sand-structured (rough) surfaces increased up to 2.46 times that of the sand-smooth interface shear resistance, which represents a 146% increase for Soil 1. For Soil 2 and Soil 3, the increases were 103% and 131%, respectively.

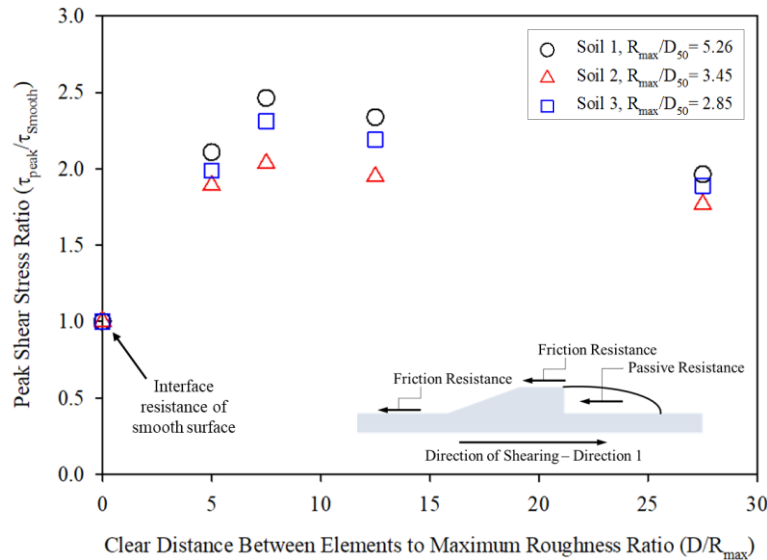


Figure 13. Relationship between soil-structured (rough) interface resistance to soil-smooth resistance with normalized distance to maximum roughness from interface tests conducted at 50 kPa normal (confining) stress on all soils

Figure 14 illustrates the relationship between the mobilized stress ratio of smooth and structured (rough) surfaces and the normal (confining) stress, referred to as the stress ratio (τ_{peak}/σ_n). As shown in Figure 14, increases in the clear distance to maximum roughness (D/R_{max}) ratio resulted in higher stress ratios for tests on all three sandy soils. For Soil 1, which has a smaller D_{50} , an initial increase in D/R_{max} from 5 to 7.5 led to a sharp rise in the mobilized stress ratio. Further increases from 7.5 to 12.5 resulted in a moderate decrease in the stress ratio and increases from 12.5 to 27.5 caused a more significant decline in the stress ratio. The trends for tests with Soil 2 (medium) and Soil 3 (coarser) sands were somewhat similar to those observed for tests with Soil 1 (finer) sand. As seen in Figure 14, the stress ratio for sand-smooth and sand-structured (rough) surfaces increased up to 0.91, while the stress ratios were 0.76 and 0.87 for Soils 2 and 3, respectively.

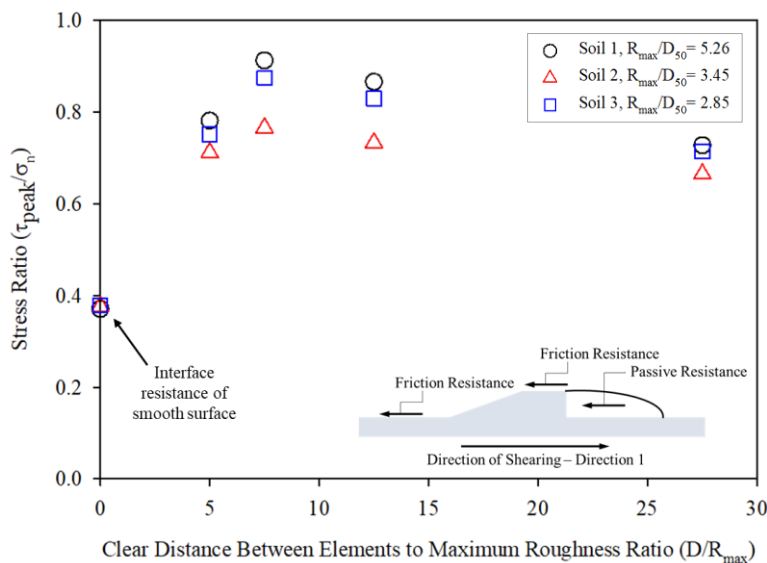


Figure 14. Relationship between soil-structured (rough) interface resistance to normal (confining) stress with normalized distance to maximum roughness from interface tests conducted at 50 kPa normal (confining) stress on all soils

As suggested by numerous studies (e.g., Uesugi & Kishida, 1986 [57]; Dietz & Lings, 2006 [52]; Dove & Frost, 1999 [3]; and Han et al., 2018 [16]), the level of surface roughness significantly influences the interface shear resistance of random surfaces. However, for surfaces with structured elements, the resistance may be controlled by the geometry and shape of the elements. The magnitude of roughness, as described by normalized roughness parameters (i.e., the average roughness $R_a = R_a/D_{avg}$ and normalized roughness $R_n = R_{max}/D_{50}$), plays a crucial role in determining interface shear resistance. Specifically, increasing the normalized roughness ($R_n = R_{max}/D_{50}$) leads to a higher interface friction angle, with an upper limit determined by the soil's internal angle of friction. The R_n values for Soils 1, 2, and 3 are 5.26, 3.45, and 2.85, respectively. These values are considered large, resulting in high mobilized interface resistance compared to the internal strength of the soil. The results summarized in Figures 13 and 14 suggest that the key parameters controlling the interface shear resistance of structured (rough) surfaces under monotonic axial loading are the surface form, roughness, and the characteristic ratio of surface elements. Additionally, these results indicate that the ratio of clear distance to maximum roughness (D/R_{max}) has a more significant impact on interface behavior than particle size or normalized roughness (R_n), as suggested by previous studies.

5. Conclusions

The experimental research presented in this article involved modifying a conventional direct shear apparatus to perform monotonic interface direct shear tests on three soil samples with different characteristics (primarily varying particle sizes). These soils were tested against five bio-inspired engineered or structured (rough) element surfaces, including a smooth surface. The experimental data on soil volume change (contraction vs. dilation) from the interface shear tests revealed differences in soil deformation mechanisms and interface strength resistance. The investigation led to the following conclusions:

- Shearing smooth (untextured) surfaces against soils with different particle sizes mobilized almost the same peak interface shear resistance due to the dominant particle sliding (frictional resistance) load transfer mechanism. However, there was a noticeable difference in the post-peak interface shear behavior. Soils with a smaller coefficient of uniformity (C_u) experienced a more pronounced reduction in interface resistance with horizontal (shearing) displacement.
- The structured (rough) surfaces with trapezoidal-like or bio-inspired-engineered elements' form, roughness, and arrangement influenced the mobilized interface shear resistance and behavior. When the element roughness level was kept constant, increasing the clear distance (D) resulted in an increase in shear resistance and soil dilation up to a maximum value. Beyond this point, further increases in D led to a decrease in mobilized resistance, accompanied by a contractive soil response. Based on the interface test results, the interface shear resistance of bio-inspired-engineered elements spaced at larger clear distances (or with fewer trapezoidal elements per unit length of contact) was expected to match the soil-smooth interface shear resistance. This behavior was consistent across all soil specimens, regardless of their characteristics and particle sizes.
- The shape of the trapezoidal-like elements enabled the mobilization of larger interface resistance (maximum attainable interface shear stress) due to the load-transfer mechanism. This mechanism consisted of frictional resistance at the top (crest) and the untextured (smooth) zones between surface elements, along with passive resistance due to the development of soil wedges at the front and back faces of the elements. The shape of the surface elements enhanced shear resistance and suggested that various geo-structures such as piles, soil anchors, nails, and conventional reinforcing elements in mechanically stabilized earth walls could benefit from such designs.
- The clear distance to maximum roughness (D/R_{max}) ratio, or surface element characteristic ratio, was found to influence and control the mobilized interface resistance and load-transfer mechanisms at the soil-structured (rough) surface interface. It was observed that only one surface, with what is termed the optimum surface element characteristic ratio (i.e., D/R_{max}), achieved the maximum interface shear resistance. This behavior was consistent in all tests conducted on the three sandy soils. Surfaces with a D/R_{max} smaller than the optimum displayed resistance mainly consisting of frictional resistance, with smaller passive resistance due to the partial development of passive wedges (i.e., rough surfaces with closely spaced elements). Conversely, surfaces with a D/R_{max} slightly larger than the optimum showed resistance from friction and larger passive wedges. When D/R_{max} was significantly larger than the optimum, the surface mainly resisted friction with minimal passive resistance (smaller passive wedges), potentially matching the interface resistance of a smooth surface. The optimum D/R_{max} corresponds to a surface that maximizes the number of fully developed passive wedges for all tested soils (1, 2, and 3).
- The results of the tests conducted as part of this study suggest that the load-transfer mechanism and mobilized interface shear resistance at the soil-structured (rough) surface interface are primarily controlled by the D/R_{max} ratio. However, normalized roughness parameters (e.g., R_n) are commonly adopted for sand-random (rough) surfaces. Future tests will focus on evaluating the influence of the clear distance to element base length ratio and its relation to the clear distance to maximum roughness ratio (D/R_{max}) on the interface shear resistance of bio-inspired-engineered surfaces.

6. Declarations

6.1. Author Contributions

Conceptualization, M.A.Q., M.F.T., and A.A.A.; methodology, M.A.Q., M.F.T., A.A.A., and R.O.A.; formal analysis, M.A.Q., M.F.T., and A.A.A.; investigation, M.A.Q., M.F.T., A.A.A., and R.O.A.; resources, M.A.Q., M.F.T., and A.A.A.; data curation, M.A.Q., M.F.T., and A.A.A.; writing—original draft preparation, M.A.Q., M.F.T., A.A.A., and R.O.A.; writing—review and editing, M.A.Q., M.F.T., A.A.A., and R.O.A.; visualization, M.A.Q.; supervision, M.A.Q.; project administration, M.A.Q. All authors have read and agreed to the published version of the manuscript.

6.2. Data Availability Statement

The data presented in this study are available in the article.

6.3. Funding

The authors received no financial support for the research, authorship, and/or publication of this article.

6.4. Acknowledgements

The authors would like to thank Eng. Mousa Falleh Alatneh and Mr. Mahmoud Nawaf Bnian from the technical staff in the Unit of Engineering Workshops at Yarmouk University for providing materials and support. The authors also would like to thank Eng. Banan Rasmi Bani Baker from the Civil Engineering Department (Geotechnical Engineering Laboratory) at Yarmouk University for her assistance during the experimentation stage.

6.5. Conflicts of Interest

The authors declare no conflict of interest.

7. References

- [1] Irsyam, M., & Hryciw, R. D. (1991). Friction and passive resistance in soil reinforced by plane ribbed inclusions. *Géotechnique*, 41(4), 485–498. doi:10.1680/geot.1991.41.4.485.
- [2] Mitchell, J. K., & Villet, W. C. (1987). Reinforcement of earth slopes and embankments. National Cooperative Highway Research Program report, Transportation Research Board, Washington, United States.
- [3] Dove, J. E., Frost, J. D., Han, J., & Bachus, R. C. (1997). The influence of geomembrane surface roughness on interface strength. *Proceedings of Geosynthetics*, 97(1), 863-876.
- [4] ardine, R.J., Lehane, B.M., Everton, S.J. (1993). Friction Coefficients for Piles in Sands and Silts. *Offshore Site Investigation and Foundation Behaviour. Advances in Underwater Technology, Ocean Science and Offshore Engineering*, 28. Springer, Dordrecht, Netherlands. doi:10.1007/978-94-017-2473-9_31.
- [5] O'Hara, K. B., & Martinez, A. (2020). Effects of Asperity Height on Monotonic and Cyclic Interface Behavior of Bioinspired Surfaces under Constant Normal Stiffness Conditions. *Geo-Congress 2020*, 243–252. doi:10.1061/9780784482834.027.
- [6] Tehrani, F. S., Han, F., Salgado, R., Prezzi, M., Tovar, R. D., & Castro, A. G. (2016). Effect of surface roughness on the shaft resistance of non-displacement piles embedded in sand. *Geotechnique*, 66(5), 386–400. doi:10.1680/jgeot.15.P.007.
- [7] Abu Qamar, M. I., & Suleiman, M. T. (2023). Evaluating the Effects of Asperity Height on Shear Strength of Cohesive Soil-Structure Interface Subjected to Monotonic and Cyclic Axial Loading, 270–280. doi:10.1061/9780784484685.028.
- [8] Dove, J. E., & Jarrett, J. B. (2002). Behavior of Dilative Sand Interfaces in a Geotribology Framework. *Journal of Geotechnical and Geoenvironmental Engineering*, 128(1), 25–37. doi:10.1061/(asce)1090-0241(2002)128:1(25).
- [9] Martinez, A., & Frost, J. D. (2017). The influence of surface roughness form on the strength of sand-structure interfaces. *Geotechnique Letters*, 7(1), 104–111. doi:10.1680/jgele.16.00169.
- [10] Uesugi, M., & Kishida, H. (1986). Frictional Resistance at Yield Between Dry Sand and Mild Steel. *Soils and Foundations*, 26(4), 139–149. doi:10.3208/sandf1972.26.4_139.
- [11] Abu Qamar, M. I., & Suleiman, M. T. (2022). Evaluating the Influence of Surface Roughness on Interface Shear Strength of Cohesive Soil-Structure Interface Subjected to Axial Monotonic Loading. *Geo-Congress 2022*, 281–291. doi:10.1061/9780784484029.028.
- [12] Kou, H. L., Diao, W. Z., Zhang, W. C., Zheng, J. B., Ni, P., Bo-An, J. A. N. G., & Wu, C. (2021). Experimental study of interface shearing between calcareous sand and steel plate considering surface roughness and particle size. *Applied Ocean Research*, 107, 102490. doi:10.1016/j.apor.2020.102490.
- [13] Hebel, G. L., Martinez, A., & Frost, J. D. (2015). Shear zone evolution of granular soils in contact with conventional and textured CPT friction sleeves. *KSCE Journal of Civil Engineering*, 20(4), 1267–1282. doi:10.1007/s12205-015-0767-6.

- [14] Sitbba Rao, K. S., Allam, M. M., & Robinson, R. G. (1998). Interfacial friction between sands and solid surfaces. *Proceedings of the Institution of Civil Engineers: Geotechnical Engineering*, 131(2), 75–82. doi:10.1680/igeng.1998.30112.
- [15] Tovar-Valencia, R. D., Galvis-Castro, A., Salgado, R., & Prezzi, M. (2018). Effect of Surface Roughness on the Shaft Resistance of Displacement Model Piles in Sand. *Journal of Geotechnical and Geoenvironmental Engineering*, 144(3), 4017120. doi:10.1061/(asce)gt.1943-5606.0001828.
- [16] Han, F., Ganju, E., Salgado, R., & Prezzi, M. (2018). Effects of Interface Roughness, Particle Geometry, and Gradation on the Sand–Steel Interface Friction Angle. *Journal of Geotechnical and Geoenvironmental Engineering*, 144(12), 4018096. doi:10.1061/(asce)gt.1943-5606.0001990.
- [17] Martinez, A., & Frost, J. D. (2017). The influence of surface roughness form on the strength of sand-structure interfaces. *Geotechnique Letters*, 7(1), 104–111. doi:10.1680/jgele.16.00169.
- [18] Mortara, G., Mangiola, A., & Ghionna, V. N. (2007). Cyclic shear stress degradation and post-cyclic behaviour from sand-steel interface direct shear tests. *Canadian Geotechnical Journal*, 44(7), 739–752. doi:10.1139/T07-019.
- [19] Porcino, D., Fioravante, V., Ghionna, V. N., & Pedroni, S. (2003). Interface behavior of sands from constant normal stiffness direct shear tests. *Geotechnical Testing Journal*, 26(3), 289–301. doi:10.1520/gtj11308j.
- [20] Fioravante, V. (2002). On the shaft friction modelling of non-displacement piles in sand. *Soils and Foundations*, 42(2), 23–33. doi:10.3208/sandf.42.2_23.
- [21] Martinez, A., Palumbo, S., & Todd, B. D. (2019). Bioinspiration for Anisotropic Load Transfer at Soil–Structure Interfaces. *Journal of Geotechnical and Geoenvironmental Engineering*, 145(10), 4019074. doi:10.1061/(asce)gt.1943-5606.0002138.
- [22] Qian, J. G., Gao, Q., Xue, J. F., Chen, H. W., & Huang, M. S. (2017). Soil and ribbed concrete slab interface modeling using large shear box and 3D FEM. *Geomechanics and Engineering*, 12(2), 295–312. doi:10.12989/gae.2017.12.2.295.
- [23] Abu Qamar, M. I., & Suleiman, M. T. (2023). Development of Cyclic Interface Shear Test Device and Testing Procedure to Measure the Response of Cohesive Soil-Structure Interface. *Geotechnical Testing Journal*, 46(3), 488–509. doi:10.1520/GTJ20210270.
- [24] Mortara, G., Mangiola, A., & Ghionna, V. N. (2007). Cyclic shear stress degradation and post-cyclic behaviour from sand-steel interface direct shear tests. *Canadian Geotechnical Journal*, 44(7), 739–752. doi:10.1139/T07-019.
- [25] O’Hara, K. B., & Martinez, A. (2020). Monotonic and Cyclic Frictional Resistance Directionality in Snakeskin-Inspired Surfaces and Piles. *Journal of Geotechnical and Geoenvironmental Engineering*, 146(11), 4020116. doi:10.1061/(asce)gt.1943-5606.0002368.
- [26] O’Hara, K. B., & Martinez, A. (2023). Cyclic axial response and stability of snakeskin-inspired piles in sand. *Acta Geotechnica*, 19(3), 1139–1158. doi:10.1007/s11440-023-02007-y.
- [27] Li, H., Yan, C., Shi, Y., Sun, W., Bao, H., & Li, C. (2024). A statistical damage model for the soil–structure interface considering interface roughness and soil shear area. *Construction and Building Materials*, 431, 136606. doi:10.1016/j.conbuildmat.2024.136606.
- [28] DeJong, J. T., Frost, J. D., & Cargill, P. E. (2001). Effect of Surface Texturing on CPT Friction Sleeve Measurements. *Journal of Geotechnical and Geoenvironmental Engineering*, 127(2), 158–168. doi:10.1061/(asce)1090-0241(2001)127:2(158).
- [29] Frost, J. D., & DeJong, J. T. (2005). In Situ Assessment of Role of Surface Roughness on Interface Response. *Journal of Geotechnical and Geoenvironmental Engineering*, 131(4), 498–511. doi:10.1061/(asce)1090-0241(2005)131:4(498).
- [30] Martinez, A., & Palumbo, S. (2018). Anisotropic Shear Behavior of Soil-Structure Interfaces: Bio-Inspiration from Snake Skin. *IFCEE 2018*, 94–104. doi:10.1061/9780784481592.010.
- [31] Prakash, B., Tiwari, A. K., Dash, S. R., & Patra, S. (2024). Structural evaluation and performance based optimization of approach slab design for mitigating bridge approach settlement through an Indian case study. *Structures*, 60, 105864. doi:10.1016/j.istruc.2024.105864.
- [32] Wang, S., Abu Qamar, M. I., Suleiman, M. T., & Vermaak, N. (2024). Evaluation of borehole interface shear test simulations for cohesive soils under monotonic loading: A comparison of Mohr–Coulomb and hypoplasticity constitutive models. *Finite Elements in Analysis and Design*, 237, 104180. doi:10.1016/j.finel.2024.104180.
- [33] Stutz, H.H., Martinez, A. (2018). Hypoplastic Simulation of Axisymmetric Interface Shear Tests in Granular Media. In: Wu, W., Yu, H.S. (eds) *Proceedings of China-Europe Conference on Geotechnical Engineering*. Springer Series in Geomechanics and Geoengineering. Springer, Cham, Switzerland. doi:10.1007/978-3-319-97112-4_16.
- [34] Zhou, W. H., Yin, J. H., & Hong, C. Y. (2011). Finite element modelling of pullout testing on a soil nail in a pullout box under different overburden and grouting pressures. *Canadian Geotechnical Journal*, 48(4), 557–567. doi:10.1139/t10-086.
- [35] Martinez, A., DeJong, J., Akin, I., Aleali, A., Arson, C., Atkinson, J., Bandini, P., Baser, T., Borela, R., Boulanger, R., Burrall, M., Chen, Y., Collins, C., Cortes, D., Dai, S., DeJong, T., Del Dottore, E., Dorgan, K., Fragaszy, R., ... Zheng, J. (2022). Bio-inspired geotechnical engineering: principles, current work, opportunities and challenges. *Géotechnique*, 72(8), 687–705. doi:10.1680/jgeot.20.p.170.

- [36] Wang, H. L., Zhou, W. H., Yin, Z. Y., & Jie, X. X. (2019). Effect of grain size distribution of sandy soil on shearing behaviors at soil–structure interface. *Journal of Materials in Civil Engineering*, 31(10), 04019238. doi:10.1061/(ASCE)MT.1943-5533.0002880.
- [37] Martinez, A. (2021). Skin Friction Directionality in Monotonically- and Cyclically-Loaded Bio-inspired Piles in Sand. *DFI Journal - The Journal of the Deep Foundations Institute*, 15(1). doi:10.37308/dfijnl.20200831.222.
- [38] O'Hara, K. B., & Martinez, A. (2024). Direction-dependent failure envelopes of sand-structure interfaces with snakeskin-inspired surfaces. *Canadian Geotechnical Journal*. doi:10.1139/cgj-2023-0522.
- [39] Martinez, A., Zamora, F., & Wilson, D. (2024). Field Evaluation of the Installation and Pullout of Snakeskin-Inspired Anchorage Elements. *Journal of Geotechnical and Geoenvironmental Engineering*, 150(8), 4024068. doi:10.1061/jggefkg.2023.12311.
- [40] DeJong, J. T., & Westgate, Z. J. (2009). Role of Initial State, Material Properties, and Confinement Condition on Local and Global Soil-Structure Interface Behavior. *Journal of Geotechnical and Geoenvironmental Engineering*, 135(11), 1646–1660. doi:10.1061/(asce)1090-0241(2009)135:11(1646).
- [41] Vafaei, N., Fakharian, K., & Sadrekarimi, A. (2021). Sand-sand and sand-steel interface grain-scale behavior under shearing. *Transportation Geotechnics*, 30, 100636. doi:10.1016/j.trgeo.2021.100636.
- [42] Vangla, P., & Latha, G. M. (2015). Influence of particle size on the friction and interfacial shear strength of sands of similar morphology. *International Journal of Geosynthetics and Ground Engineering*, 1, 1-12. doi:10.1007/s40891-014-0008-9.
- [43] Namjoo, A. M., Baniasadi, M., Jafari, K., Salam, S., Toufigh, M. M., & Toufigh, V. (2022). Studying effects of interface surface roughness, mean particle size, and particle shape on the shear behavior of sand-coated CFRP interface. *Transportation Geotechnics*, 37, 100841. doi:10.1016/j.trgeo.2022.100841.
- [44] ASTM D5321/D5321M1. (2021). D5321-12 Standard Test Method for Determining the Shear Strength of Soil-Geosynthetic and Geosynthetic-Geosynthetic Interfaces by Direct Shear. ASTM International, Pennsylvania, United States. doi:10.1520/D5321_D5321M-21.
- [45] DeJong, J. T., Randolph, M. F., & White, D. J. (2003). Interface load transfer degradation during cyclic loading: A microscale investigation. *Soils and Foundations*, 43(4), 81–93. doi:10.3208/sandf.43.4_81.
- [46] Martinez, A., & Stutz, H. H. (2019). Rate effects on the interface shear behaviour of normally and over consolidated clay. *Geotechnique*, 69(9), 801–815. doi:10.1680/jgeot.17.P.311.
- [47] ASTM D6913/D6913M-17 (2021). Standard Test Methods for Particle-Size Distribution (Gradation) of Soils Using Sieve Analysis. ASTM International, Pennsylvania, United States. doi:10.1520/D6913_D6913M-17.
- [48] ASTM D2487-17e1. (2020). Standard Practice for Classification of Soils for Engineering Purposes (Unified Soil Classification System). ASTM International, Pennsylvania, United States. doi:10.1520/D2487-17E01.
- [49] ASTM D3080/D3080M-11. (2020). Standard Test Method for Direct Shear Test of Soils Under Consolidated Drained Conditions. ASTM International, Pennsylvania, United States. doi:10.1520/D3080_D3080M-11.
- [50] Westgate, Z. J., & DeJong, J. T. (2023). Role of Initial State, Material Properties, and Confinement Condition on Local and Global Soil–Structure Interface Behavior during Cyclic Shear. *Journal of Geotechnical and Geoenvironmental Engineering*, 149(10), 04023088. doi:10.1061/JGGEFK.GTENG-11306.
- [51] Jiang, M., Dai, Y., Cui, L., Shen, Z., & Wang, X. (2014). Investigating mechanism of inclined CPT in granular ground using DEM. *Granular Matter*, 16, 785-796. doi:10.1007/s10035-014-0508-2.
- [52] Dietz, M. S., & Lings, M. L. (2006). Postpeak Strength of Interfaces in a Stress-Dilatancy Framework. *Journal of Geotechnical and Geoenvironmental Engineering*, 132(11), 1474–1484. doi:10.1061/(asce)1090-0241(2006)132:11(1474).
- [53] Frost, J. D., DeJong, J. T., & Recalde, M. (2002). Shear failure behavior of granular-continuum interfaces. *Engineering Fracture Mechanics*, 69(17), 2029–2048. doi:10.1016/S0013-7944(02)00075-9.
- [54] Hryciw, R. D., & Irsyam, M. (1993). Behavior of sand particles rigid ribbed inclusions during shear. *Soils and Foundations*, 33(3), 1–13. doi:10.3208/sandf1972.33.3_1.
- [55] Kishida, H., & Uesugi, M. (1987). Tests of the interface between sand and steel in the simple shear apparatus. *Géotechnique*, 37(1), 45–52. doi:10.1680/geot.1987.37.1.45.
- [56] Potyondy, J. G. (1961). Skin friction between various soils and construction materials. *Geotechnique*, 11(4), 339–353. doi:10.1680/geot.1961.11.4.339.
- [57] Uesugi, M., & Kishida, H. (1986). Influential Factors of Friction Between Steel and Dry Sands. *Soils and Foundations*, 26(2), 33–46. doi:10.3208/sandf1972.26.2_33.
- [58] Tehrani, F. S., Han, F., Salgado, R., & Prezzi, M. (2017). Laboratory Study of the Effect of Pile Surface Roughness on the Response of Soil and Non-Displacement Piles (pp. 256–264). doi:10.1061/9780784480465.027.